

Mouse T Cell Membrane Proteins Rt6-1 and Rt6-2 Are Arginine/Protein Mono(ADPribosyl)transferases and Share Secondary Structure Motifs with ADP-ribosylating Bacterial Toxins*

(Received for publication, November 20, 1995, and in revised form, January 17, 1996)

Friedrich Koch-Nolte^{†§¶}, David Petersen[‡], Sriram Balasubramanian[‡], Friedrich Haag[§], Dominik Kahlke[§], Thomas Willer[§], Robert Kastelein[‡], Fernando Bazan[‡], Heinz-Günter Thiele^{‡§¶}

From the [‡]DNAX Research Institute of Molecular & Cellular Biology, Palo Alto, California 94304 and the [§]Department of Immunology, University Hospital, D-20246 Hamburg, Federal Republic of Germany

Mono ADP-ribosylation is a posttranslational protein modification that has been implicated in the regulation of key biological functions in bacteria as well as in animals. Recently, the first cDNAs for eucaryotic mono(ADPribosyl)transferases were cloned and found to exhibit significant sequence similarity only to one other known protein, the T cell differentiation antigen Rt6. In this paper we describe secondary structure analyses of Rt6 and related proteins and show conserved structure motifs and amino acid residues consistent with a common ancestry of these eucaryotic proteins and bacterial ADP-ribosyltransferases. Moreover, we have expressed soluble mouse Rt6-1 and Rt6-2 gene products in which C-terminal tags (FLAG-His₆) replace the native glycosylphosphatidylinositol anchor signal sequences. Purified recombinant Rt6-2, but not Rt6-1, shows NAD⁺ glycohydrolase activity, which is inhibited by the arginine analogue agmatine. Immunoprecipitation of recombinant Rt6-1 and Rt6-2 with anti-FLAG M2 antibody followed by incubation with [³²P]NAD⁺ leads to rapid and covalent incorporation of radioactivity into the light chain of the M2 antibody. The bound label is resistant to treatment with HgCl₂ but sensitive to NH₂OH, characteristic of arginine-linked ADP-ribosylation. These results demonstrate that Rt6-1 and Rt6-2 possess the enzymatic activities typical for NAD⁺-dependent arginine/protein mono(ADPribosyl)transferases (EC 2.4.2.31). They are the first such enzymes to be molecularly characterized in the immune system.

Mono ADP-ribosylation is a posttranslational protein modification in which the ADP-ribose (ADPR)¹ moiety of NAD⁺ is transferred from NAD⁺ to a specific amino acid residue in a target protein, while the nicotinamide moiety is released (1, 2). The reaction is catalyzed by a family of amino acid-specific ADP-ribosyltransferases, which includes some of the most po-

tent bacterial toxins such as diphtheria and cholera toxins. These toxins interfere with cellular functions by catalyzing mono ADP-ribosylation of key cellular target proteins in their human hosts, such as elongation factor EF2 and the α subunit of heterotrimeric G-proteins. The crystal structure has been determined for four of the bacterial toxins, revealing a highly conserved core surrounding the presumptive active site crevice (3–6). In case of diphtheria toxin, the co-crystallized NAD⁺ analogue ApUp was observed to bind in this crevice (7). These findings support the concept that all bacterial toxins with ADP-ribosyltransferase activity have a common fold of the catalytic site in spite of highly divergent amino acid sequences (8). *In vitro*, many of the bacterial toxins can modify proteins other than their physiologic targets and, in the absence of target protein, some toxins can use water as an alternative acceptor resulting in the hydrolysis of NAD⁺ to nicotinamide and ADPR, which can be measured as NAD⁺ glycohydrolase activity.

Ample biochemical evidence has shown that endogenous mono ADP-ribosylation reactions occur also in animal tissues (9–12). Recent findings suggest that this posttranslational protein modification may be used to control important endogenous physiological functions such as the induction of long term potentiation in the brain, terminal muscle cell differentiation, and the cytotoxic activity of killer T cells (13–16). Recently, the first eucaryotic ADP-ribosyltransferases were purified and sequenced from rabbit skeletal muscle and chicken bone marrow (17, 18). The primary sequences of these eucaryotic proteins encode glycosylphosphatidylinositol (GPI)-anchored membrane proteins with entirely extracellular polypeptide chains. Homology searches (17, 18) revealed significant sequence similarity of the muscle and bone marrow enzymes to a similarly GPI-anchored T cell membrane protein RT6 (19, 20). Limited amino acid sequence identities to bacterial toxins have also been noted (21, 22).

RT6, originally discovered in the rat as a T cell alloantigen (23), is a T cell differentiation and activation antigen (24, 25). Its expression is restricted to peripheral T cells and intraepithelial lymphocytes of the gut (24, 26). Molecular cloning showed that RT6 antigens are encoded by a single copy gene in the rat with two known, remarkably divergent alleles (designated *RT6^a* and *RT6^b*) (27, 20) and by two closely linked genes in the mouse (designated *Rt6-1* and *Rt6-2*) (28). *Rt6-1* and *Rt6-2* have conserved open reading frames, and the deduced amino acid sequences are 78.5% identical (28). A defect in the development of RT6/Rt6-expressing cells coincides with increased susceptibility for autoimmune disease in different animal models (29, 30). In the first study of RT6 enzyme activity, Takada *et al.* (21) reported that rat RT6 displays NAD⁺ glycohydrolase activity but, in contrast to the skeletal muscle enzyme, does not modify arginine analogues. This led to the

* This work was supported in part by Grants Ko1144 and No310 from the Deutsche Forschungsgemeinschaft (to F.K.-N.). DNAX is fully supported by Schering Plough Corporation. The costs of publication of this article were defrayed in part by the payment of page charges. This article must therefore be hereby marked "advertisement" in accordance with 18 U.S.C. Section 1734 solely to indicate this fact.

[¶] To whom correspondence may be addressed: Dept. Immunol., Medical Clinic, University Hospital, D-20246 Hamburg, FRG. Tel.: 49-40-4717 3612; Fax: 49-40-4717 4243.

¹ The abbreviations used are: ADPR, adenosine diphosphate ribose; GPI, glycosylphosphatidylinositol; G-protein, guanine nucleotide-binding protein; PLC, phospholipase C; PI-PLC, phosphatidylinositol-specific PLC; M2L, M2 antibody light chain; PAGE, polyacrylamide gel electrophoresis; TBS, Tris-buffered saline; PBS, phosphate-buffered saline; Tricine, N-[2-hydroxy-1,1-bis(hydroxymethyl)ethyl]glycine; FPLC, fast protein liquid chromatography; CTL, cytotoxic T cell.

provisional classification of RT6 as a NAD⁺ glycohydrolase rather than an ADP-ribosyltransferase (21, 22). More recently, Haag *et al.* (31) and Maehama *et al.* (32) showed that rat RT6 is capable of arginine-linked automodification, although modification of heterologous target proteins by rat RT6 was not demonstrated.

The mono(ADPribosyl)transferases share their NAD⁺ glycohydrolase activity with another family of NAD⁺ metabolizing enzymes, the ADP-ribosylcyclases, which include the lymphocyte surface proteins CD38 (33) and BST-1/BP-3 (34, 35). These enzymes catalyze the conversion of NAD⁺ into cyclic ADP-ribose (cADPR) and nicotinamide. They differ somewhat in their relative NAD⁺ glycohydrolase versus ADPR cyclase activities. The physiological function of the ADP-ribosylcyclases is at present still unclear.

To characterize further the relationship of Rt6 and known mono(ADPribosyl)transferases we have performed secondary structure prediction analyses of Rt6 and related vertebrate proteins. Moreover, we have expressed soluble versions of mouse Rt6-1 and Rt6-2 and report here the molecular characterization and enzymatic properties of these recombinant proteins. The results show that these proteins, indeed, should be classified as arginine/protein mono(ADPribosyl)transferases (EC 2.4.2.31).

EXPERIMENTAL PROCEDURES

Materials—[adenylate-³²P]NAD⁺ (5000 Ci/mol) and secondary antibodies were purchased from Amersham Corp. NAD⁺ glycohydrolase from *Neurospora crassa* and arginine-rich histones were purchased from Sigma; phosphatidylinositol-specific phospholipase C (PI-PLC) from *Bacillus thuringiensis* was from Immunotech. The M2 monoclonal antibody specific for the eight-amino acid FLAG tag (36) and M2-antibody Sepharose were from Kodak/IBI; a His₆ tag-specific monoclonal antibody and nickel nitrilotriacetic acid-agarose were from Qiagen.

Amino Acid Sequence Alignment and Secondary Structure Prediction Analyses—Multiple sequence alignment was performed with a weighted dynamic programming method (HSSP/MaxHom) (37). The generated multiple alignment was used as input for secondary structure predictions that were produced by profile-based neural network systems (PHDsec) (38).

Generation of Rt6-specific Antisera and Affinity Purification of Rt6-specific Antibodies—Preparation and purification of antisera will be detailed elsewhere (28). In brief, the synthetic peptide (KAPQLLED-FNMNEE), corresponding to amino acid residues 48–62 of mouse Rt6-1 and Rt6-2, was coupled to ovalbumin. Immunizing a rabbit with this compound led to antiserum K48, immunizing a rat with purified recombinant Rt6-2-glutathione *S*-transferase fusion protein to antiserum R2.

Expression of C-terminally Tagged Soluble Rt6 in Insect Cells—For cloning into the *Xba*I and *Bgl*II cloning sites of the baculovirus transfer vector pMLHT (39), appropriate *Rt6-1* and *Rt6-2* cDNA fragments were polymerase chain reaction-amplified from cloned cDNA with fusogenic primers 1BF (TTA GCC TCT AGA ATG CCA TCA AAT AAT TTC AAG TTC), 2BR (GTG ACC AGA TCT GCT ATA GAA GCA ATT AAA GTT GCT), and 3BR (GTG ACC AGA TCT ATT ATA GAA GCA ATT GAA GTT GCT). Polymerase chain reaction products were digested with *Xba*I and *Bgl*II and cloned into pMLHT. Sf9 insect cells were cotransfected with the recombinant transfer vector and Baculovirus Gold genomic DNA (Pharmingen). Cell supernatants were harvested 4 days after transfection, diluted, and viral plaques were grown on agarose-suspended Sf9 cells. A single viral plaque was used to infect 10⁷ insect cells. Infected cells were resuspended in 4 ml of culture medium and propagated at 27 °C. Supernatants were harvested 5 days later, and 1 ml of supernatant was used to infect 10⁸ Sf9 cells. Infected cells were propagated in 50-ml spinner cultures, and supernatants were harvested after 4–5 days.

Recombinant protein was purified by affinity chromatography either on M2-antibody Sepharose (Kodak/IBI) or nickel nitrilotriacetic acid-agarose (Qiagen) columns according to the manufacturers' instructions. Columns were washed extensively with TBS, 0.1% Triton X-100, and bound protein was eluted with 50 mM glycine-HCl, pH 2.5 (M2 column), or 100 mM imidazol (nickel nitrilotriacetic acid column). Acid-eluted material was immediately neutralized with 1 M Tris, pH 8.0. Protein

concentration was estimated by comparison of Coomassie-stained bands in SDS-polyacrylamide gels using a dilution series of lysozyme as a standard.

Preparation and Analysis of PI-PLC Supernatants from Mouse Cells—Cell suspensions (10⁸ white cells/ml) from spleens of 6-week-old female BALBc/ByJ, C57BL/6J, or NZW/LacJ mice were incubated for 1 h at 37 °C in RPMI 1640 medium (Life Technologies, Inc.) containing 1 unit of PI-PLC (Jackson). Cells were pelleted by centrifugation, and supernatants were either used directly or stored at –20 °C.

SDS-PAGE and Western Blot Analyses—Total protein was precipitated from cell supernatants with Strataclean-Resin (Stratagene). FLAG-tagged fusion proteins were precipitated with M2-antibody Sepharose beads (Kodak/IBI) (36). Precipitates were washed in PBS and resuspended in SDS-PAGE sample buffer. All samples were heated for 5 min at 95 °C and cleared by centrifugation before loading onto 10 or 12% polyacrylamide gels. SDS-PAGE was performed in Tris-glycine or Tricine buffer as described previously (19). Fractionated proteins were blotted onto nitrocellulose (Amersham Corp.) or polyvinylidene difluoride (Applied Biosystems) membranes.

For silver staining, blots were submerged in freshly prepared staining solution (0.1 ml of 20% (w/v) silver nitrate added dropwise to a solution of 0.5 ml of 40% (w/v) sodium citrate, 0.4 ml of 20% (w/v) ferric sulfate, and 9 ml of H₂O). Blots were washed in water after bands became visible (usually after 0.5–5 min).

For immunostaining, blots were blocked with 10% goat serum in TBS and incubated for 2–16 h at 4 °C with primary antibody at appropriate dilutions (K48 serum at 1:2000, affinity-purified K48 antibodies at 1:10, M2 antibody at 1 μg/ml) in TBS, 0.5% Tween-20 (TBST), 10% goat serum and washed extensively in TBST. Secondary reagents for detection of bound K48 were biotinylated goat anti-rabbit Ig (1:2000, Amersham Corp.) and streptavidin peroxidase (1:5,000, Amersham Corp.); for detection of bound M2-antibody peroxidase-labeled donkey anti-mouse Ig (1:5,000, Amersham Corp.). After washing in TBST, bound antibody was detected with the ECL system (Amersham Corp.) according to the manufacturer's instructions and by exposure to Amersham ECL films. For detection of bound ³²P, the blots were subjected to autoradiography by exposure to a Kodak X-Omat AR film for 12–16 h at –80 °C.

Enzyme Assays—For analysis of NAD⁺ glycohydrolase activity, purified Rt6 or CD38 (the latter a kind gift of J. C. Grimaldi, DNAX Institute) were suspended at 20 μg/ml in 10 mM Tris, pH 7.4, and reactions (20 μl) initiated by addition of cold NAD⁺ (1 mM). Samples were incubated for 30–90 min at 37 °C, frozen in dry ice, and analyzed by anion-exchange chromatography on a fast flow Source Q resin column using a Pharmacia Biotech Inc. FPLC system. Products were eluted with a salt gradient and detected by adsorption at 280 nm with the Pharmacia UV-2 detector.

For analysis of ADP-ribosyltransferase activity, purified Rt6 or Rt6 precipitated from Sf9 cell supernatants with M2-antibody affinity matrix was suspended in 50 μl of PBS (0.2 μg Rt6/ml) containing 2 μCi of [³²P]NAD⁺ (5000 Ci/mol, Amersham Corp.) or 2 μCi of [³²P]ADPR. The latter was prepared by incubating 2 μCi of [³²P]NAD⁺ in 50 μl of PBS with 0.1 milliunit of *N. crassa* NAD⁺ glycohydrolase (Sigma) for 30 min at 37 °C; complete conversion of [³²P]NAD⁺ to [³²P]ADPR was verified by thin-layer chromatography. Labeling reactions were carried out for 30 min at 37 °C. After labeling, affinity matrix-associated protein was precipitated by centrifugation. Soluble protein was precipitated with Strataclean-Resin (Stratagene) (10 μl/reactions) according to the manufacturer's instructions. Precipitates were washed extensively with PBS and then suspended in either PBS, 10 mM NAD⁺, 10 mM HgCl₂, 1 M NaCl, or 1 M NH₂OH, and incubated on a tumbler overnight at room temperature. Precipitates were then again pelleted by centrifugation and subjected to SDS-PAGE analyses as described above.

RESULTS

Secondary Structure Predictions of Rt6-1, Rt6-2, and Related Proteins—The amino acid sequences of mouse *Rt6-1* and *Rt6-2* were aligned with those of related proteins from rat, rabbit, human, and chicken with the HSSP/MaxHom program, and the resulting multiple alignment was used as input for secondary structure predictions with the PHDsec program (see Fig. 1A) (38, 37). While the N-terminal portion (residues 1–115) of these proteins is predicted to be mainly helical, the C-terminal region (residues 115–225) is dominated by β-sheets and a single prominent helix. This pattern of β-sheets, interrupted by a single helix, is quite similar to the pattern of secondary

structure motifs predicted by PHDsec for bacterial mono(ADP-ribose)transferases (not shown). In case of *Escherichia coli* heat labile enterotoxin and pertussis toxin, the predicted secondary structures match well with those in the known crystal structures of these toxins (4, 6) (illustrated schematically in Fig. 1B). Recognizable amino acid sequence similarities occur throughout the region of predicted structural homology to the bacterial toxins. The degree of sequence similarity is highest in the secondary structure units that line the active site crevice in the bacterial toxins (Fig. 1C). Note in particular that three highly conserved amino acid residues occur in a similar context of predicted secondary structure units in the eucaryotic proteins as in the bacterial toxins (residues *R* = Arg¹²⁶, *S* = Ser¹⁴⁷, and *E* = Glu¹⁸⁴, in $\beta 1$, $\beta 3$ - $\alpha 3$, and $\beta 6$, respectively, Fig. 1, A and B). In case of the bacterial toxins, the glutamic acid residue in $\beta 6$ has been implicated as a key catalytic residue by photoaffinity labeling with NAD⁺ (40, 41) and by site-directed mutagenesis (42, 43). The arginine residue in $\beta 1$ and the serine residue in $\beta 3$ are linked by a hydrogen bond in *E. coli* and pertussis toxins and may play a role in maintaining the conformation of the active site (these residues are histidine and tyrosine, respectively, in pseudomonas and diphtheria toxins, see Fig. 1C) (4, 8, 6). Site-directed mutagenesis studies indicate that these residues also are essential for enzymatic activity of the bacterial toxins (44–46).

Expression of Soluble Rt6-1 and Rt6-2 in Sf9 Insect Cells—For expression of soluble tagged Rt6-1 and Rt6-2, appropriate cDNA fragments were cloned into a baculovirus expression vector, replacing the GPI-anchor signal sequences with C-terminal tags (FLAG-His₆) (illustrated schematically in Fig. 2). Fig. 3, A and B, show SDS-PAGE and immunoblot analyses of supernatants from Sf9 insect cells infected with plaque-purified baculoviruses. The results show that infected insect cells secrete proteins of 27–30 kDa (corresponding to those predicted for the Rt6-1 and Rt6-2 polypeptide chains) that are recognized by the FLAG tag-specific monoclonal antibody M2 (Fig. 3A). The same bands are recognized by Rt6 peptide-specific antiserum K48 (Fig. 3B, lanes 1 and 2), and the reactivity of the bands with K48 is blocked completely by the cognate peptide (Fig. 3B, lanes 4 and 5). Note that Rt6-2 in Sf9 supernatants consistently appears more heterogeneous than Rt6-1 (Fig. 3A lanes 7–12 versus lanes 1–5 and Fig. 3B, lane 2 versus lane 1). Recombinant Rt6-1 and Rt6-2 were readily purified from Sf9 supernatants by affinity chromatography on M2-Sepharose or nickel nitrilotriacetic acid-agarose columns (not shown).

Comparing Recombinant Rt6 with Rt6 Released by PI-PLC from Spleen Cells Indicates That the Latter Is Subject to More Extensive Posttranslational Modification—Fig. 4 shows a comparative immunoblot analysis of Rt6 gene products secreted by

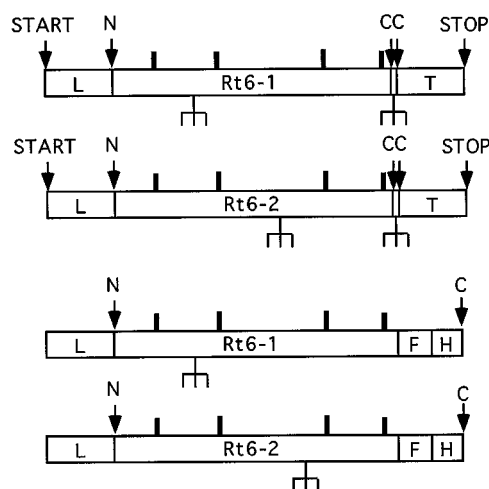


FIG. 2. Schematic diagram of native Rt6 and expression constructs. Native Rt6-1 and Rt6-2 coding sequences (top) are compared with those of recombinant constructs for expressing tagged protein in the baculovirus system (bottom). *L*, posttranslationally cleaved N-terminal leader signal sequence for translocation to the endoplasmic reticulum; *T*, posttranslationally cleaved C-terminal tail signal sequence for GPI-anchor attachment; *F*, FLAG tag-binding site for monoclonal antibody M2; *H*, His₆ tag-binding site for metal chelating resin; *N*, N terminus of native Rt6 generated by cleavage of *L*; *CC*, potential C termini of native Rt6 generated by cleavage of *T*. The precise position of the cleavage site in mouse Rt6 is not known. At the position homologous to the cleavage site determined in rat RT6.2 by sequencing of the C-terminal peptide (54), mouse Rt6 contains insertions of 7 (Rt6-1) and 9 (Rt6-2) amino acid residues. *C*, C terminus of recombinant Rt6 resulting from a stop codon following *F* and *H*. *Forks* indicate potential N-linked glycosylation sites; *boldface lines* indicate four cysteine residues conserved in the known eucaryotic transferases.

Sf9 cells (lanes 4 and 5) or released from mouse spleen cells by treatment with PI-PLC (lanes 1–3). The quantity of Rt6 contained in 1 μ l of Sf9 cell supernatant corresponds roughly to that released by PI-PLC from 5×10^6 spleen cells. The results show that Rt6 released from spleen cells by PI-PLC migrates more slowly than that produced by insect cells, possibly reflecting differences in posttranslational modifications in the two cell systems. The reactivity of the bands in PI-PLC supernatants with K48 antibodies was fully blocked by the cognate peptide (not shown), indicating that these bands indeed correspond to Rt6. This conclusion is supported by the fact that the same pattern of bands is detected with antiserum R2 raised by immunizing a rat with recombinant glutathione *S*-transferase-Rt6 (not shown). Notice the doublet of Rt6 bands from BALB/c mice (Fig. 4, lane 1) versus the distinctive single Rt6 bands from C57 and NZW mice (lanes 2 and 3). This phenomenon is

be superimposed with an root-mean-square difference of 1.6 Å in the known structures of *E. coli* heat labile enterotoxin, pertussis toxin, diphtheria toxin, and pseudomonas exotoxin A (3–5, 8, 6). The presumptive active site crevice is lined by $\beta 1$, $\beta 3$ - $\alpha 3$, and $\beta 6$. The conserved catalytic glutamic acid residue in $\beta 6$, which can be cross-linked to NAD⁺ by photoaffinity labeling in all four toxins, is marked by *E*. The conserved arginine residue in $\beta 1$ and the conserved serine residue in $\beta 3$, which interact via a hydrogen bond in the *E. coli* and pertussis toxins are marked by *R* and *S* (note that these residues are histidine and tyrosine in pseudomonas and diphtheria toxins, see C). C, alignment of residues lining the active site crevice in bacterial toxins of known three-dimensional structure with similar sequences in other ADP-ribosyltransferases. Nomenclature of conserved secondary structure units is as in A and B. The four bacterial toxins with known three-dimensional structures are marked by ● on the right. Distinct subfamilies are separated by horizontal lines. Members of each subfamily show significant sequence similarities (>20% overall sequence identity). Residues conserved in at least three distinct subfamilies are boxed. The presumptive catalytic arginine, serine, and glutamic acid residues are marked by arrows on the bottom. Residues in the eucaryotic enzymes that occur also in at least three of the six subfamilies of bacterial enzymes are marked by an asterisk on the bottom. *ETA*, *Pseudomonas* exotoxin A; *DT*, diphtheria toxin; *DRR*, *Rhodospirillum rubrum* dinitrogenase reductase ADP-ribosyltransferase; *DAB*, *Azospirillum brasiliense* ADP-ribosyltransferase; *DRC*, *Rhodospirillum capsulatus* ADP-ribosyltransferase; *LT*, *E. coli* heat labile enterotoxin; *PT*, pertussis toxin; *CT*, cholera toxin; *MTX*, *Bacillus sphaericus* mosquitocidal toxin; *ETS*, *Pseudomonas* exotoxin S; *C3C* and *C3D*, *Clostridium botulinum* type C and type D phage exoenzymes C3; *EDIN*, epidermal cell differentiation inhibitor from *Staphylococcus aureus*; *T2* and *T4*, gpALT ADP-ribosyltransferase from *E. coli* bacteriophages T2 and T4; *rRT6*, rat T cell marker; *Rt6*, *mRt6-1*, and *mRt6-2*, mouse T cell markers Rt6-1 and Rt6-2; *rMAT* and *hMAT*, rabbit and human skeletal muscle ADP-ribosyltransferases; *chBMA1* and *chBMA2*, chicken bone marrow ADP-ribosyltransferases 1 and 2. Sequences for vertebrate proteins are as in A; sequences for bacterial and bacteriophage proteins were compiled from Genbank accession numbers: K01995 (*ETA*), P00588 (*DT*), P14299 (*DRR*), M87319 (*DAB*), X71131 (*DRC*), P06717 (*LT*), P04977 (*PT*), P01555 (*CT*), S27514 (*MTX*), L27629 (*ETS*), Q00901 (*C3C*), P15879 (*C3D*), P24121 (*EDIN*), X69893 (*T2*), and X15811 (*T4*).

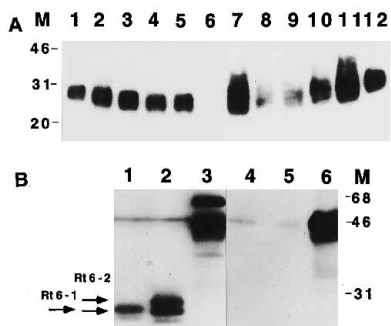


FIG. 3. Western blot analysis of recombinant Rt6 in insect cell supernatants. A, supernatants (20 μ l/lane) from Sf9 cells infected with six individual plaque-purified Rt6-1- and Rt6-2-encoding baculoviruses (lanes 1-6 and 7-12, respectively) were subjected to SDS-PAGE and Western blot analyses. The blot was immunostained with FLAG tag-specific mouse monoclonal antibody M2, peroxidase-labeled secondary antibody, and the ECL detection system (Amersham Corp.). The blot was exposed for 1 s to Kodak X-Omat AR film. B, Sf9 cell supernatants (2 μ l/lane) were subjected to SDS-PAGE and Western blot analysis as in A. The blot was immunostained with Rt6 peptide-specific rabbit serum K48 in the absence (lanes 1-3) or presence (lanes 4-6) of cognate peptide 48 (10 μ g/ml), peroxidase-labeled secondary antibody, and the ECL detection system (Amersham Corp.). Lanes 1 and 4, Rt6-1-containing supernatant; lanes 2 and 5, Rt6-2-containing supernatant; lanes 3 and 6, rainbow *M*₁ marker (Amersham Corp.). Note that K48, which was raised against Rt6 peptide coupled to ovalbumin, reacts with ovalbumin both in the absence (lane 3) and presence (lane 6) of peptide 48. Arrows indicate bands corresponding to recombinant Rt6 proteins.

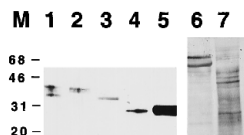


FIG. 4. Comparative Western blot analyses of recombinant Rt6-1 and Rt6-2 from Sf9 cells and native Rt6-1 and Rt6-2 released from mouse spleen cells by PI-PLC. Spleen cells from BALBc/ByJ (lane 1), C57BL/6J (lane 2), and NZW/LacJ (lane 3) mice were treated with PI-PLC. Rt6-1- and Rt6-2-containing (lanes 4 and 5) Sf9 cell supernatants were prepared as in Fig. 2C. Proteins were precipitated from cleared supernatants with Strataclean resin and subjected to SDS-PAGE and Western blot analysis. The blot was immunostained with affinity-purified K48 antibodies, peroxidase-labeled secondary antibody, and the ECL detection system (Amersham Corp.). PI-PLC supernatants were from 0.5×10^7 cells (lanes 1 and 2) and 2×10^7 cells (lane 3); lanes 4 and 5 each contain 1 μ l of insect cell supernatant. The blot was exposed to Kodak X-Omat AR film for 8 s. Control lanes with Rt6-1-containing Sf9 cell supernatant (lane 6) and C57BL/6 mouse spleen cell PI-PLC supernatant (lane 7) were silver-stained for total protein.

consistent with strain-specific differences in the relative levels of *Rt6-1* and *Rt6-2* gene expression observed by RT-PCR (C57BL/6 mice do not express *Rt6-1*, NZW mice do not express *Rt6-2*) (30, 28). After treatment with reducing agents, the Rt6 bands in spleen and insect cell supernatants show similar shifts in M_r (not shown), indicating the presence of disulfide bonds in both.

Recombinant Rt6-2 but Not Rt6-1 Hydrolyses NAD^+ —Purified recombinant Rt6-1 and Rt6-2 were incubated for up to 90 min with NAD^+ , and the reaction products were analyzed by FPLC (Fig. 5). The results show that Rt6-2 catalyzes the hydrolysis of NAD^+ to nicotinamide and ADPR (Fig. 5, A-C), whereas no NAD^+ glycohydrolase activity could be detected for Rt6-1 (Fig. 5D).

The hydrolysis of NAD^+ by Rt6-2 was not affected by the addition of 10 mM histidine or 10 mM asparagine but was inhibited in a dose-dependent manner by the arginine analogue agmatine (Fig. 6). The addition of 10 mM agmatine almost

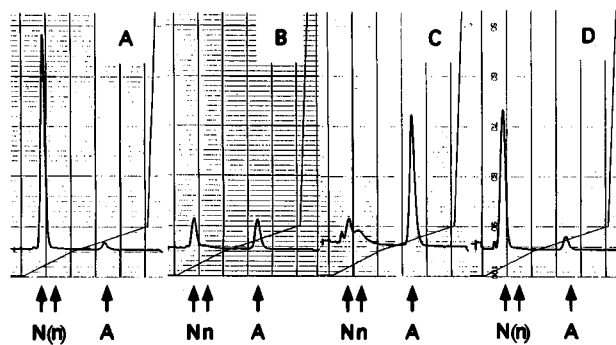


FIG. 5. FPLC analyses of the reaction products after incubation of purified recombinant Rt6-1 and Rt6-2 with NAD^+ . Purified recombinant Rt6-1 (panel D) and Rt6-2 (panels A-C) were incubated with 1 mM NAD^+ for 0-90 min at 37 $^{\circ}$ C. Reaction products were analyzed by FPLC on a fast flow Source Q resin (Pharmacia) column, and products were detected by absorption at 280 nm. The elution points of markers *N* (NAD^+), *n* (nicotinamide), and *A* (ADPR) are indicated on the bottom. A, Rt6-2, 0 min; B, Rt6-2, 30 min; C, Rt6-2, 90 min; D, Rt6-1, 90 min.

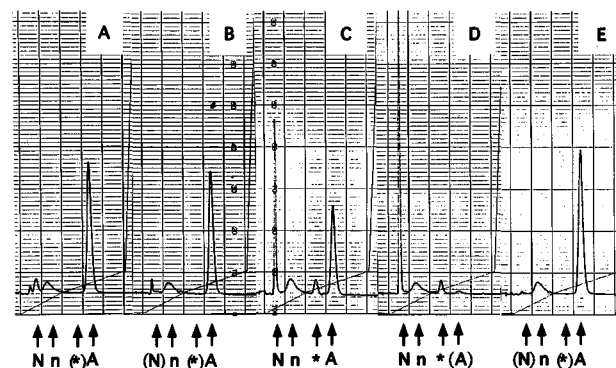


FIG. 6. FPLC analyses of the reaction products after incubation of purified recombinant Rt6-2 and CD38 with NAD^+ . Purified recombinant Rt6-2 (panels A-D) and CD38 (panel E) were incubated with 1 mM NAD^+ for 90 min at 37 $^{\circ}$ C in the presence of 10 mM asparagine (A), 10 mM histidine (B), 10 mM agmatine (C), or 10 mM agmatine (D and E). Supernatants were analyzed by FPLC as in Fig. 5. The elution points of markers are indicated as in Fig. 5. A peak of absorbance possibly representing ADPR-agmatine is marked with an asterisk.

completely blocked the hydrolysis of NAD^+ by Rt6-2 but not that of recombinant CD38 (an ADP-ribosylcyclase) (Fig. 6, D versus E). Note the appearance of an additional peak of absorbance in the samples containing Rt6-2 and agmatine (marked by asterisks in Fig. 6, C and D) but not in that containing CD38 and agmatine (Fig. 6E). The nature of this peak is not known but possibly represents ADPR-agmatine.

Recombinant Rt6-1 and Rt6-2 Bound to M2 Sepharose Beads Catalyze ADP-ribosylation of the M2 Light Chain (M2L)—Incubation of recombinant Rt6-1 and Rt6-2 immunoprecipitated by FLAG tag-specific M2 antibody beads with [32 P] NAD^+ for 30 min at 37 $^{\circ}$ C leads to incorporation of radiolabel into matrix-associated protein. These proteins and appropriate controls were analyzed by SDS-PAGE immunoblot analysis (Fig. 7, top panels) and autoradiography (Fig. 7, bottom panels). Note that the reagents used for immunostaining recognize only Rt6 in crude insect cell supernatants (Fig. 7, lane 1, see also Fig. 3). However, in samples containing the M2 antibody, they react also with the faster migrating M2 light chain (M2L) (e.g. Fig. 7, lanes 3 and 6, M2 antibody beads alone, and Fig. 7, lanes 2, 4, 7, and 8, Rt6-containing immunoprecipitates on M2 antibody beads). The results reveal that radiolabel incorporated from [32 P] NAD^+ into Rt6-1 and Rt6-2 immunopre-

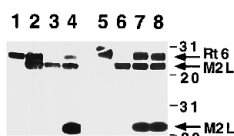


FIG. 7. SDS-PAGE analyses of immunoprecipitated recombinant Rt6-1 and Rt6-2 labeled with [32 P] NAD $^{+}$. Sf9 cell supernatant, purified Rt6, M2 Sepharose, and Rt6/M2 immunoprecipitates were incubated for 30 min at 37 °C in the absence (lanes 1 and 2) or presence (lanes 3–8) of [32 P]NAD $^{+}$. Samples were subjected to SDS-PAGE and immunoblot analysis with antiserum K48 and the ECL system as in Fig. 3 (top panel). For autoradiography, the blots were then covered with a black sheet of paper to quench remaining chemiluminescence and exposed to Kodak X-Omat AR film for 16 h at –80 °C (bottom panel). Lane 1, crude Sf9 cell supernatant containing recombinant Rt6-1; lane 2, Rt6-1/M2 immunoprecipitate (no radiolabel); lanes 3 and 6, M2 Sepharose beads; lane 4, Rt6-1/M2 immunoprecipitate obtained from crude Sf9 cell supernatant; lane 5: purified Rt6-2; lane 7, purified Rt6-2 reprecipitated with M2 beads; lane 8, Rt6-2/M2 immunoprecipitate from crude Sf9 cell supernatant. Bands corresponding to Rt6 and the light chain of the M2 antibody are marked by arrows.

cipitates is covalently associated (*i.e.* SDS-resistant) with M2L but not with Rt6 itself (Fig. 7, lanes 4, 7, and 8). Labeling is Rt6-dependent since M2 beads alone do not incorporate any label (Fig. 7, lanes 3 and 6). Moreover, labeling is NAD $^{+}$ -dependent since incubation of Rt6/M2 precipitates with [32 P]ADPR does not lead to incorporation of any label (not shown). Note also that incubation of Rt6 alone with [32 P]NAD $^{+}$ does not lead to incorporation of any label (Fig. 7, lane 5).

Radiolabel Associated with M2L Is Sensitive to Hydroxylamine Consistent with Linkage to Arginine—To determine the nature of the linkage of the radiolabel to M2L, immunoprecipitates labeled by Rt6-1 (Fig. 8A) and Rt6-2 (Fig. 8B) were incubated under conditions known to cleave specifically the linkage of ADPR to thiol groups (10 mM HgCl $_2$) or to arginine (1 M neutral NH $_2$ OH) (47, 48). The M2L-bound label is resistant to overnight treatment with PBS (lanes 1), 10 mM NAD $^{+}$ (lanes 2), 1 M NaCl (lanes 3), and 10 mM HgCl $_2$ (lane 5), but sensitive to treatment with 1 M NH $_2$ OH (lane 4). Arginine-rich histones are also readily ADP-ribosylated by recombinant Rt6-1 and Rt6-2, and here, too, bound label is sensitive to NH $_2$ OH but resistant to HgCl $_2$ (not shown). Radiolabel released by NH $_2$ OH was identified as [32 P]ADPR (not shown). These results strongly suggest that Rt6-catalyzed mono ADP-ribosylation of M2L and histones occurred at arginine residues.

DISCUSSION

The findings presented in this paper demonstrate that mouse Rt6-1 and Rt6-2 are GPI-anchored NAD $^{+}$ -dependent arginine-specific mono(ADPribosyl)transferases. They are the first such enzymes to be molecularly characterized in the immune system. Our results show that these T cell membrane proteins exhibit predicted secondary structure motifs and enzymatic activities similar to those of ADP-ribosylating bacterial toxins. The data are compatible with a distant evolutionary relationship of Rt6 and related eucaryotic membrane proteins and ADP-ribosylating bacterial toxins. This raises some interesting questions.

The results of our secondary structure prediction analyses confirm alignments made previously between eucaryotic and procaryotic transferases on the basis of amino acid sequence similarities around Glu 184 (21, 22) and considerably extend the region of predicted structural homology. It is of note that the predicted catalytic domain is encompassed entirely in the β -sheet-rich C-terminal half of the eucaryotic proteins (Fig. 1). The prediction that Glu 184 plays a catalytic role is supported by the finding that site-directed mutation of this residue almost

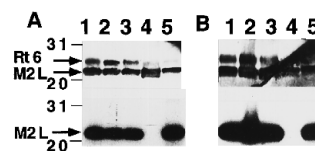


FIG. 8. Sensitivity of incorporated radiolabel to hydroxylamine. The M2L chain in Rt6-1- and Rt6-2-containing immunoprecipitates (panels A and B, respectively) was radiolabeled by incubation of beads with [32 P]NAD $^{+}$ as in Fig. 7. After extensive washing, beads were suspended in PBS (lanes 1), 10 mM NAD $^{+}$ (lanes 2), 1 M NaCl (lanes 3), 1 M NH $_2$ OH (lanes 4), or 10 mM HgCl $_2$ (lanes 5) and incubated overnight at room temperature. Beads were pelleted by centrifugation and boiled in SDS-PAGE sample buffer for 5 min before loading onto the gel. Immunoblot analyses with antiserum K48 and the ECL system (top panels) and autoradiography of the same blots (bottom panels) were performed as in Fig. 7.

completely abolishes enzyme activities of mouse Rt6 2 as has also been observed in case of the muscle enzyme (22). The significance of the additional, mainly helical, section in the N-terminal half of the eucaryotic proteins is presently unknown and open for speculation. Interesting possibilities include roles in ligand binding or translocation across the cell membrane.

The enzymatic activities of recombinant soluble Rt6-1 and Rt6-2 are characteristic for NAD $^{+}$ -dependent arginine-specific mono(ADPribosyl)transferases. This includes their capacity to ADP-ribosylate arginine in nonphysiological target proteins (Figs. 7 and 8) as well as their different NAD $^{+}$ glycohydrolase activities (Figs. 4 and 5). In the case of arginine-specific bacterial toxins, ADP-ribosylation of the physiological target is most efficient, but in its absence, other proteins, such as arginine-rich histones, can also be modified (1, 2). This property is shared by the Rt6 proteins, which also readily ADP-ribosylate arginine-rich histones but not bovine serum albumin or many other control proteins (not shown).

Interestingly, a His $_6$ tag-specific antibody (Qiagen), which is of the same isotype as the M2 antibody, does not serve as a target for ADP-ribosylation by Rt6 (not shown). Presumably, the M2 light chain contains an arginine residue in a setting suitable for modification by Rt6, which the His $_6$ tag-specific antibody lacks. Moreover, it is possible that the high local concentration of enzyme and target on the surface of the Sepharose beads is responsible for the high efficiency of the reaction with the M2 antibody. In any case, this system will provide a simple tool for analyzing Rt6 mutants, *e.g.* in identifying essential residues by site-directed mutagenesis. Moreover, it will be interesting to see whether FLAG-tagged versions of other transferases can also modify the M2 light chain or whether this is a peculiar property of the tagged Rt6 proteins.

Considering that the two mouse Rt6 proteins are just slightly more similar to one another than either is to rat RT6 (79 versus 71–73% sequence identity), it is intriguing that these proteins show such striking differences in enzymatic activities. Remarkably, neither arginine-rich histones nor the M2 antibody serve as substrates for ADP-ribosylation by FLAG-tagged recombinant rat RT6.1 or RT6.2 alloantigens (not shown). Moreover, the latter show much stronger NAD $^{+}$ glycohydrolase and, in case of RT6.2, automodification activities than do the mouse Rt6 proteins (not shown). The reason for these differences is unresolved. With the availability of recombinant RT6/Rt6 proteins, a molecular dissection of the structural domains and critical amino acid residues responsible for the observed differences in NAD $^{+}$ glycohydrolase, automodification, and arginine-ADP-ribosyltransferase activities should now be possible.

² F. Koch-Nolte, F. Haag, K. Bredehorst, J. Schröder, H. G. Thiele, manuscript in preparation.

Of course, it is obvious that neither the M2 light chain nor histones are the physiological target proteins for Rt6. The fact that Rt6 does efficiently modify these artificially presented targets indicates that it may be difficult to distinguish ADP-ribosylation of physiologically relevant targets from ADP-ribosylation of irrelevant targets *in vitro*. Certainly, caution is warranted when interpreting modifications observed *in vitro*, e.g. upon incubation of intact cells or cell lysates with radioactive NAD⁺.

The physiological target proteins of Rt6 and its eucaryotic relatives presently remain unknown. The fact that the identified eucaryotic ADP-ribosyltransferases are GPI-anchored membrane proteins raises the intriguing and as yet unresolved question whether these enzymes have extra- or intracellular targets. If they target intracellular proteins as do their bacterial toxin cousins, the question arises as to their mechanism of entry into the cytoplasm. If they have extracellular targets as some evidence seems to suggest, how is access to the required substrate NAD⁺ assured, considering that NAD⁺ is a classic intracellular metabolite and that cell membranes are impermeable to NAD⁺? A dying cell is one potential source for extracellular NAD⁺, as is a hypothetical specific secretory mechanism akin to that recently discovered for ATP, another "classic intracellular metabolite" (49). On the other hand, it is also conceivable that there exists a mechanism for translocating the eucaryotic ectoenzymes to the cytoplasm analogous to that used by bacterial toxins.

In the case of the muscle cell membrane-associated ADP-ribosyltransferase activity, *in vitro* studies have put forward evidence for modifications of both extra- and intracellular target proteins. Incubation of intact mouse muscle cells with [³²P]NAD⁺ results in arginine-linked ADP-ribosylation of several protein bands, the most prominent of which has been identified as the muscle cell-specific $\alpha 7$ integrin chain (14). Incubation of the membrane fraction from rabbit or canine muscle cells with [³²P]NAD⁺ also leads to labeling of several protein bands (50, 51). In the canine system, the intracellular G α subunit of the G_s protein regulating adenylate cyclase was identified as the most efficient target for arginine-linked ADP-ribosylation (51). G_s proteins and $\alpha 7$ integrin are thought to play important roles in signal transduction and cell-matrix interaction, respectively, and it is conceivable although not yet established that the observed target protein modifications alter physiologically relevant cellular functions.

In the case of T cell membrane-associated enzyme activity, modification of several distinct bands by arginine ADP-ribosylation has been observed after incubation of lymphoma cells and activated mouse cytotoxic T cells (CTLs) with exogenous [³²P]NAD⁺ (52, 16). Although these potential target proteins have not been defined in molecular terms, interesting functional consequences of cell surface ADP-ribosylation were observed in case of the CTLs. Thus, treatment of activated CTLs with ecto-NAD⁺ led to a dramatic suppression of the ability of these cells to proliferate in response to stimulator cells and to lyse target cells (16). Moreover, treatment of the CTLs with PI-PLC released the activity that catalyzes ADP-ribosylation of cell surface proteins and rendered the cells refractory to the suppressive effects of ecto NAD⁺. It is quite possible that the GPI-anchored enzyme activity detected by Wang *et al.* (16) corresponds to Rt6. If so, and if suppression of CTL functions by Rt6 acting on extracellular NAD⁺ and cell surface proteins were physiologically relevant, this would provide a basis for explaining the observed coincidences between defects in Rt6 gene structure and/or expression and enhanced susceptibility for autoimmune diseases in different animal models (29, 30). It is conceivable, for example, that interference with Rt6-mediated

regulation of CTL functions could lead to enhanced T cell autoreactivity. In this context it is of interest to note that treatment of NOD mice with antibodies specific for integrin $\alpha 4$, a T cell-specific relative of the most prominent target for surface ADP-ribosylation in skeletal muscle cells, has recently been shown to markedly suppress progression to autoimmune disease (53). It is tempting to speculate that the function of $\alpha 4$ integrin is affected similarly by these antibodies as by hypothetical Rt6-catalyzed ADP-ribosylation.

These exciting observations have opened a new field of experimental investigation at the interface of enzymology and immunology. The soluble, enzymatically active recombinant Rt6 proteins described here provide valuable new experimental tools to address interesting questions, e.g. what are the physiological target protein(s) of the Rt6 proteins, what is the structural basis for their enzymatic activity, and how can we probe for the possible immunomodulating activities of these reagents? Thus, it may be expected that these reagents will help shed light on the biological significance of the endogenous relatives of ADP-ribosylating bacterial toxins in animal tissues. Appropriate experiments are underway in our laboratories.

Acknowledgments—These studies were prompted by F. B., who recognized secondary structure similarities between RT6 and bacterial toxins. F. K.-N. thanks DNAX for the generous hospitality during his stay as a visiting scientist in R. K.'s laboratory. We thank Maren Kühl and Roman Gierisch for excellent technical assistance.

REFERENCES

- Jacobson, M. K., and Jacobson, E. L. (1989) *ADP-Ribose Transfer Reactions: Mechanisms and Biological Significance*. New York, Springer Verlag
- Moss, J., and Vaughan, M. (1990) *ADP-Ribosylating Toxins and G Proteins: Insights Into Signal Transduction*. Washington DC, American Society for Microbiology
- Allured, V. S., Collier, R. J., Carrol, S. F., and McKay, D. B. (1985) *Proc. Natl. Acad. Sci. U. S. A.* **83**, 1320–1324
- Sixma, T. K., Pronk, S. E., Kalk, K. H., Wartna, E. S., van Zanten, B., Witholt, B., and Hol, W. G. (1991) *Nature* **351**, 371–377
- Choe, S., Bennett, M. J., Fujii, G., Curmi, P. M., Kantardjieff, K. A., Collier, R. J., and Eisenberg, D. (1992) *Nature* **357**, 216–222
- Stein, P., Boodhoo, A., Armstrong, G. D., Cockle, S. A., Klein, M. H., and Read, R. J. (1994) *Structure Curr. Biol.* **2**, 45–57
- Weiss, M. S., Blanke, S. R., Collier, R. J., and Eisenberg, D. (1995) *Biochemistry* **34**, 773–781
- Domenighini, M., Magagnoli, C., Pizzi, M., and Rappuoli, R. (1994) *Mol. Microbiol.* **14**, 41–50
- Yost, D., and Moss, J. (1983) *J. Biol. Chem.* **258**, 4926–4929
- Godeau, F., Bellin, D., and Koide, S. S. (1984) *Anal. Biochem.* **137**, 287–296
- Peterson, J. E., Larew, J. S. A., and Graves, D. J. (1990) *J. Biol. Chem.* **265**, 17062–17069
- Maehama, T. K., Takahashi, K., Ohoka, Y., Otsuka, T., Ui, M., and Katada, T. (1991) *J. Biol. Chem.* **266**, 10062–10065
- McMahon, K. K., Piron, K. J., Ha, V. T., and Fullerton, A. T. (1993) *Biochem. J.* **293**, 789–793
- Zolkiewska, A., and Moss, J. (1993) *J. Biol. Chem.* **268**, 25273–25276
- Schuman, E. M., Meffert, M. K., Schulman, H., and Madison, D. V. (1994) *Proc. Natl. Acad. Sci. U. S. A.* **91**, 11958–11962
- Wang, J., Nemoto, E., Kots, A. Y., Kaslow, H. R., and Dennert, G. (1994) *J. Immunol.* **153**, 4048–4058
- Zolkiewska, A., Nightingale, M. S., and Moss, J. (1992) *Proc. Natl. Acad. Sci. U. S. A.* **89**, 11352–11356
- Tsuchiya, M., Hara, N., Yamada, K., Osago, H., and Shimoyama, M. (1994) *J. Biol. Chem.* **269**, 27451–27457
- Koch, F., Thiele, H. G., and Low, M. G. (1986) *J. Exp. Med.* **164**, 1338–1343
- Koch, F., Haag, F., Kashan, A., and Thiele, H. G. (1990) *Proc. Natl. Acad. Sci. U. S. A.* **87**, 964–967
- Takada, T., Iida, K., and Moss, J. (1994) *J. Biol. Chem.* **269**, 9420–9423
- Takada, T., Iida, K., and Moss, J. (1995) *J. Biol. Chem.* **270**, 541–544
- Butcher, G. W., and Howard, J. C. (1977) *Rat News Letter* **1**, 12–14
- Thiele, H. G., Koch, F., and Kashan, A. (1987) *Transplant. Proc.* **19**, 3157–3160
- Wonigeit, K., and Schwizner, R. (1987) *Transplant. Proc.* **19**, 296–298
- Fangmann, J., Schwizner, R., and Wonigeit, K. (1991) *Eur. J. Immunol.* **21**, 753–760
- Haag, F., Koch, F., and Thiele, H. G. (1990) *Nucleic Acids Res.* **18**, 1047
- Koch-Nolte, F., Haag, F., Hollmann, C., Schlott, M., Damaske, A., Bertuleit, H., Matthes, M., Kühl, M., and Thiele, H. G. *Mol. Immunol.*, in press
- Greiner, D. L., Mordes, J. P., Handler, E. S., Angelillo, M., Nakamura, N., and Rossini, A. A. (1987) *J. Exp. Med.* **166**, 461–475
- Koch-Nolte, F., Klein, J., Hollmann, C., Kühl, M., Haag, F., Gaskins, H. R., Leiter, E. H., and Thiele, H. G. (1995) *Int. Immunol.* **7**, 883–890
- Haag, F., Andresen, V., Karsten, S., Koch-Nolte, F., and Thiele, H.-G. (1995) *Eur. J. Immunol.* **25**, 2355–2361

32. Maehama, T., Nishina, H., Hoshino, S., Kanaho, Y., and Katada, T. (1995) *J. Biol. Chem.* **270**, 22747–22751
33. Howard, M., Grimaldi, J. C., Bazan, J. F., Lund, F. E., Santos, A. L., Parkhouse, R. M., Walseth, T. F., and Lee, H. C. (1993) *Science* **262**, 1056–1059
34. Dong, C., Wang, J., Neame, P., and Cooper, M. D. (1994) *Int. Immunol.* **6**, 1353–1360
35. Kaisho, T., Ishikawa, J., Oritani, K., Inazawa, J., Tomizawa, H., Muraoka, O., Ochi, T., and Hirano, T. (1994) *Proc. Natl. Acad. Sci. U. S. A.* **91**, 5325–5329
36. Hopp, T. P., Prickett, K. S., Price, V., Libby, R. T., March, C. J., Cerretti, P., Urdal, D. L., and Conlon, P. J. (1988) *Bio/Technology* **6**, 1205–1210
37. Sander, C., and Schneider, R. (1994) *Nucleic Acids Res.* **22**, 3597–3599
38. Rost, B., and Sander, C. (1993) *Proc. Natl. Acad. Sci. U. S. A.* **90**, 7558–7562
39. Grimaldi, J. C., Balasubramanian, S., Kabra, N. H., Shanafelt, A., Bazan, J. F., Zurawski, G., and Howard, M. C. (1995) *J. Immunol.* **155**, 811–817
40. Carrol, S. F., and Collier, R. J. (1984) *Proc. Natl. Acad. Sci. U. S. A.* **81**, 3307–3311
41. Barbieri, J. T., Mende-Meuller, L. M., Rappuoli, R., and Collier, R. J. (1989) *Infect. Immunol.* **57**, 3549–3554
42. Tweten, R. K., Barbieri, J. T., and Collier, R. J. (1985) *J. Biol. Chem.* **260**, 10392–10394
43. Antoine, R., Tallett, A., van Heyningen, S., and Loch, C. (1993) *J. Biol. Chem.* **268**, 24149–24155
44. Burnette, W. N., Cieplak, W., Mar, V. L., Kaljot, K. T., Sato, H., and Keith, J. M. (1988) *Science* **242**, 72–74
45. Papini, E., Schiavo, G., Sandona, D., Rappuoli, R., and Montecucco, C. (1989) *J. Biol. Chem.* **264**, 12385–12388
46. Blanke, S. R., Huang, K., Wilson, B. A., Papini, E., Covacci, A., and Collier, R. J. (1994) *Biochemistry* **33**, 5155–5161
47. Payne, D. M., Jacobson, E. L., Moss, J., and Jacobson, M. K. (1985) *Biochemistry* **24**, 7540–7549
48. Meyer, T., Koch, R., Fanick, W., and Hilz, H. (1988) *Biol. Chem. Hoppe Seyler* **369**, 579–583
49. Evans, R. J., Derkach, V., and Surprenant, A. (1992) *Nature* **357**, 503–505
50. Klebl, B. M., Matsushita, S., and Pette, D. (1994) *FEBS Lett.* **342**, 66–70
51. Quist, E. E., Coyle, D. L., Vasan, R., Satumtira, N., Jacobson, E. L., and Jacobson, M. K. (1994) *J. Mol. Cell. Cardiol.* **26**, 251–260
52. Soman, G., Haregewoin, A., Hom, R. C., and Finberg, R. W. (1991) *Biochem. Biophys. Res. Commun.* **176**, 301–308
53. Yang, X. D., Michie, S. A., Tisch, R., Karin, N., Steinman, L., and McDevitt, H. (1994) *Proc. Natl. Acad. Sci. U. S. A.* **91**, 12604–12608
54. Kashan, A., Buck, F., Haag, F., Koch, F., and Thiele, H. G. (1989) *Immunol. Lett.* **23**, 133–138